Reliability Assessment of Meshed DC Shipboard Power Systems Using Stochastic Simulation

Van Der Sande, Robin; Shekhar, Aditya; Bauer, Pavol

DOI
10.1109/ICDCM60322.2024.10664918

Publication date
2024

Document Version
Final published version

Published in
Proceedings of the 2024 IEEE Sixth International Conference on DC Microgrids (ICDCM)

Reliability Assessment of Meshed DC Shipboard Power Systems using Stochastic Simulation

Robin van der Sande
dept. Electrical Sustainable Energy
Delft University of Technology
Delft, The Netherlands
R.P.J.vanderSande@tudelft.nl

Aditya Shekhar
dept. Electrical Sustainable Energy
Delft University of Technology
Delft, The Netherlands
A.Shekhar@tudelft.nl

Pavol Bauer
dept. Electrical Sustainable Energy
Delft University of Technology
Delft, The Netherlands
P.Bauer@tudelft.nl

2024 IEEE Sixth International Conference on DC Microgrids (ICDCM) | 979-8-3503-6363-0/24/$31.00 ©2024 IEEE | DOI: 10.1109/ICDCM60322.2024.10664918

***Abstract*—In DC shipboard power systems (DC-SPS), the enhanced network complexity and high penetration of power electronic devices make the system level reliability a critical design aspect. This paper proposes a stochastic framework for the reliability assessment of DC-SPSs based on a three-stage Monte Carlo (MC) simulation, including component failure sampling, active fault propagation, and reliability index calculation. The proposed MC framework is verified for a simplified meshed DC grid through comparison with an analytical method. Later, the advantages of the MC method are demonstrated for a dynamic positioning vessel equipped with a ring-type DC power system architecture. The results quantify the impact of redundancy on the reliability of a DC-SPS, show the spread in the subsystem repair times, and reveal the system's availability during both the initialization and steady-state. Combined, the simulation results reveal the strengths and weaknesses of the designed grid, guiding the focus for future reliability enhancements.**

***Index Terms*—Reliability, Shipboard power systems, DC grid, Monte Carlo**

I. Introduction

In 2023, the International Maritime Organization (IMO) published a strategy on reducing the greenhouse gas emissions of international shipping, striving to cut emission levels by at least 70 % in 2040, ultimately reaching net-zero around 2050 [1]. When addressing this maritime challenge, the all-electric ship (AES) is a commonly proposed solution as it can improve the vessel's efficiency, incorporate renewable energy sources, and enhance ship automation [2], [3]. The basis of an AES is the shipboard power system (SPS), which serves as the interconnecting grid between the electric vessel loads and the generation modules, combining the functionality of the traditionally split electric power and propulsion power system. Although AESs can be implemented with both DC and AC power systems, a DC-SPS provides significant advantages in efficiency, power density, source synchronization, and energy storage system (ESS) integration [4]–[8]. However, the enhanced network complexity of DC grids combined with the high penetration of PE converters can significantly compromise the system's reliability [9]. Especially given that the harsh environmental conditions of ships, including vibrations, humidity, and salinity, enhance component degradation and rise failure uncertainty [10], [11].

The authors are with the department of Electrical Sustainable Energy in the DCE&S Group at Delft University of Technology. This work was supported by the Dutch research council (NWO) and is a contribution towards the research project: KICH1.VE02.20.007 on survivable DC power systems for ships.

As the functionality of the SPS is vital to both the vessel mission and crew safety, ensuring its reliability is critical for the adoption of the DC-AES. In literature, multiple analytical methods are posed for the SPS reliability assessment, including minimum cut sets [12], fault tree analysis [13]–[16], Markov models [17], and the reliability block diagram (RBD) [18]. These analytical methods are fast to apply for small-sized DC grids, though become complex for larger more intricate power systems, often requiring significant assumptions to cope with operating conditions [19]. Moreover, these analytical methods lack flexibility in application, making the reliability comparison of different SPS designs difficult and time-consuming. Stochastic simulation methods, like Monte Carlo (MC), are widely used for the adequacy assessment of utility power systems [20], [21] and DC microgrids [22]–[24]. Although more computationally intensive, the MC method provides significant advantages such as: estimating both the expected value and distribution of a reliability index, incorporating nonelectrical system factors such as the weather effects in the assessment, and including the impact of system processes like reconfiguration, maintenance, and protection [19]. Overall, MC simulation can incorporate a more detailed model of the SPS while keeping flexibility in design, making the reliability comparison of SPS topologies simpler and more accurate.

In the present work, a Monte Carlo framework is developed for the reliability assessment of DC-SPSs. This framework is verified using a simplified meshed DC grid and then applied to a complex DC-SPS to analyze its reliability. The rest of this paper is organized as follows: Section II introduces the multi-stage MC framework for the DC-SPS reliability assessment. Section III applies this concept to assess a ring-type DC-SPS of a wind turbine installation vessel. Finally, the conclusions are drawn in Section IV.

II. Methodology

The reliability of a power system $R_{\mathrm{s}}(t)$ is defined as the probability that the system functions adequately throughout the operating period $[0, t]$ under the intended operating conditions [25]. Like any power system, the DC-SPS's reliability is determined by its components (PE converters, protection

equipment, distribution cables) and its network structure [16]. The failure character of a component can be described in three stages: the infant stage, the normal operating stage, and the wear-out stage. When considering a component in the normal operating stage, its failure rate λ can be assumed to be constant, giving the reliability function (1) throughout the useful lifetime [26]. This simplification assumes that the component's systematic failures related to the debugging and manufacturing process have been mitigated while wear-out failures associated with internal component degradation have yet to become predominant [27].

$$R(t) = e^{-\lambda t} \tag{1}$$

To assess the system reliability $R_{\mathrm{s}}(t)$, the failure characteristics of the interconnected components must be combined according to the defined network structure. This adequacy assessment can be performed using a MC simulation, which analyses the stochastic failure behavior of the system through a set of simulation evaluations, also known as trails or experiments [28]. These simulations emulate the operating process of the SPS while incorporating the uncertainty in component functionality through a set of random variables (RV). Throughout the simulations, these RVs are sampled from their probability distributions, corresponding to the failure and repair rates, representing the randomness in component failure and repair times. The result of each simulation is then compiled into a reliability index sample. When the number of simulations N is large enough, the law of large numbers dedicates that the average of the reliability index samples converges to the expected value [29]. Consequently, reflecting the adequacy of the assessed power system. The MC simulation framework for the reliability assessment of DC-SPSs is provided in Fig. 1. This framework is structured in three main stages which are: component failure sampling, system simulation, and reliability index calculation.

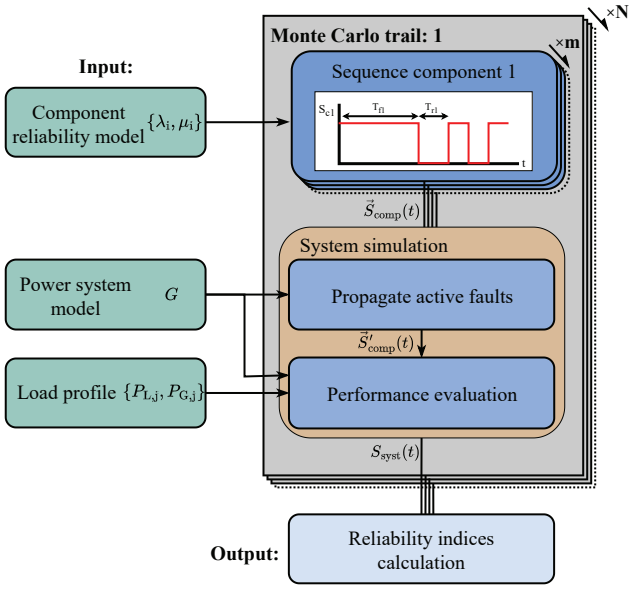

Fig. 1. Monte Carlo framework for reliability assessment of DC-SPSs.

A. Component failure sampling

The first stage of the MC framework uses the component failure and repair rates $\{\lambda_i, \mu_i\}$ to create the failure sequence samples $S_{ci}(t)$ of the m components in the SPS. For the operation of the DC-SPS, it is assumed that each component can either function in the up-state or fail in the down-state. The up-to-down state transition occurs with the component failure rate λ_i while and down-to-up state transition occurs with the repair rate μ_i. In which μ is the inverse of the component's mean time to repair (MTTR). The failure sequence sample $S_{ci}(t)$ is then constructed as a concatenation of RV realizations, alternating between 1 and 0 based on the time to failure $T_f \sim \mathrm{Exp}(\lambda_i)$ and time to repair $T_r \sim \mathrm{Exp}(\mu_i)$ samples, as given in (2).

$$S_{ci}(t) = \begin{cases} 1 & \text{for } t < T_{f,1} \\ 0 & \text{for } T_{f,1} \le t < T_{f,1} + T_{r,1} \\ 1 & \text{for } T_{f,1} + T_{r,1} \le t < T_{f,1} + T_{r,1} + T_{f,2} \\ 0 & \text{for } \cdots \end{cases} \tag{2}$$

Once a failure sequence has been sampled for all m components in the system, the component functionality vector $\vec{S}_{comp}(t)$ as in (3) is passed to the system simulation.

$$\vec{S}_{comp}(t) = [S_{c1}(t), S_{c2}(t), S_{c3}(t), \cdots, S_{cm}(t)] \tag{3}$$

B. System simulation

The second stage of the MC framework simulates the operation of the DC-SPS given the component functionalities $\vec{S}_{comp}(t)$ and the network graph model G. Fig. 2(a) provides an example of a DC shipboard power subsystem feeding a single load from two fully redundant generators through a pair of switchboards and transmission lines. Given this notional SPS, the graph model can be constructed as in Fig. 2(b),

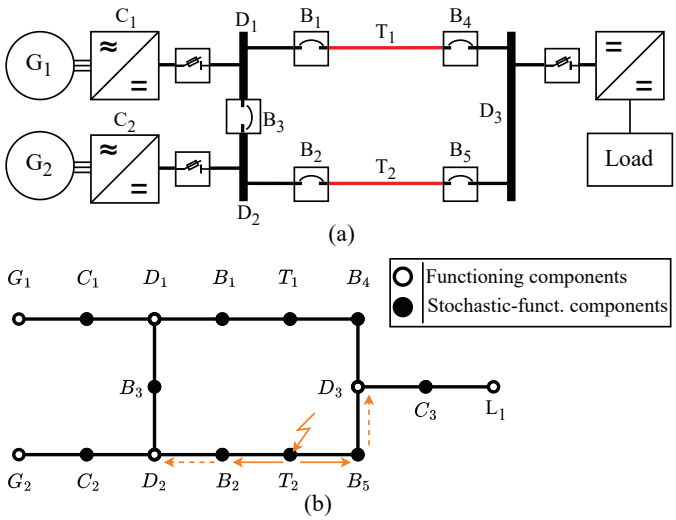

Fig. 2. Notional DC shipboard power subsystem with (a) the model diagram and (b) the corresponding graph model.

where the black nodes indicate components with stochastic functionality, while the white nodes are assumed to be fully functional components. Note that this functioning character of the load and generator modules is imposed to focus the reliability assessment on solely reflecting the impact of the power system's design.

As a component (e.g. PE converter) is constructed by interconnecting devices (IGBTs, diodes, capacitors), it can encounter multiple failure modes. As introduced in [30], component failure events can be split into active failures and passive failures. A passive failure is represented by an open circuit, which does not impact the remaining healthy components in the system. In contrast, an active failure acts like a short circuit, causing the fault to propagate from the component through the adjacent power lines and tripping the neighboring protection devices. Optimally, a circuit breaker (CB) would always trip upon detecting an active fault. However, practically, in a fraction f_{cb} of the cases, the circuit breaker is stuck or fails to act accordingly [16].

To address the active and passive failure behavior in the MC framework, the stochastic active fault propagation is implemented, altering $\vec{S}_{\text{comp}}(t)$. Upon an active failure of a SPS component, the functionalities of all CBs are sampled using uniform random variables $U_{\text{cb,k}} \sim \text{U}(0,1) > f_{\text{cb}}$. Based on this sampling, the active fault is propagated through the power system as shown in Fig. 2(b) for an active fault in the distribution cable T_2. Then, combining the components passive and propagated active failure sequences defines the alerted component functionality vector $\vec{S}'_{\text{comp}}(t)$.

Based on $\vec{S}'_{\text{comp}}(t)$, the MC method evaluates the system performance $S_{\text{syst}}(t)$ given the operational requirements of the vessel. Note that each vessel has a unique performance objective and, therefore, its own supply requirements for the different loads in the SPS. Consequently, the performance evaluation depends heavily on the application and characteristics of the considered vessel. $S_{\text{syst}}(t)$ is then defined as 1 and 0 at times the DC-SPS meets and fails to meet the supply requirements. To determine the adequacy of the SPS, a wide range of methods can be used, ranging from a simple connectivity study to a load flow analysis based on the operation profile $\{P_{\text{L,j}}, P_{\text{G,j}}\}$ [26]. It should be noted that the latter approach significantly raises the required computational effort of the MC simulation and is therefore not further discussed in this paper.

C. Reliability index calculation

The final stage of the MC framework uses the system performances $S_{\text{syst}}(t)$ of the N simulation evaluations to determine a reliability index estimate. Analyzing $S_{\text{syst}}(t)$ of each MC trail provides a reliability index sample, like a service interruption rate sample $\lambda_{\text{s,n}}$, a total downtime sample $D_{\text{s,n}}$, or a system reliability sample $R_{\text{s,n}}(t)$. The average of these N samples gives the reliability index estimate of the MC simulation. For the provided subsystem of Fig. 2(a), the system is said to be functional ($S_{\text{syst}}(t) = 1$) if the load module is connected to at least one of the two generators. The system reliability sample

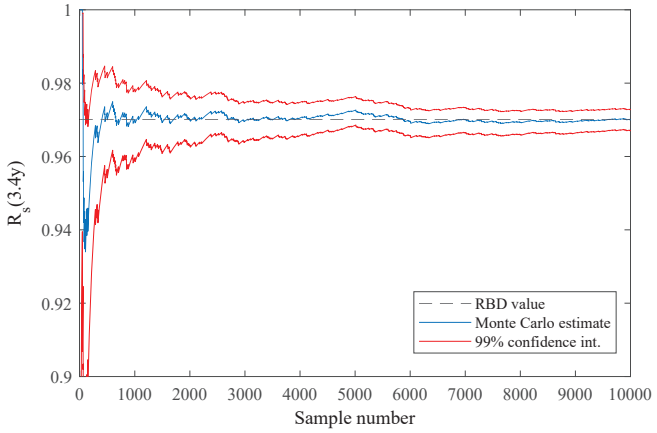

Fig. 3. Monte Carlo simulated system reliability after 3.4 years of operation plotted as a function of the sample size and compared to the RBD value.

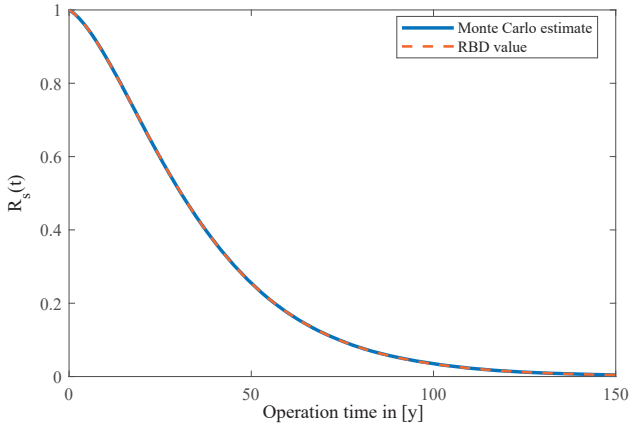

Fig. 4. The Monte Carlo estimated system level reliability curve in comparison to the RBD value for 300k samples.

$R_{\text{s,n}}(t)$ is then defined as in (4), providing the system reliability estimate as in (5).

$$R_{\text{s,n}}(t) = \begin{cases} 1 & \text{for } t < \min\left(t \,|\, S_{\text{syst}}(t) = 0\right) \\ 0 & \text{else} \end{cases} \tag{4}$$

$$\hat{R}_{\text{s}}(t) = \frac{1}{N} \sum_{n=1}^{N} R_{\text{s,n}}(t) \tag{5}$$

D. MC method verification

To verify the workings of the proposed MC simulation framework, its results are compared to an analytical approach. With this comparison, the subsystem of Fig. 2(a) is assumed to contain unrepairable components that solely encounter passive failures with a breaker failure rate $\lambda_{\text{b}} = 0.01\,\#/\text{y}$, a transmission line failure rate $\lambda_{\text{t}} = 0.01\,\#/\text{y}$, and a converter failure rate $\lambda_{\text{c}} = 0.006\,\#/\text{y}$. Following the reliability block diagram method, the system level reliability can be defined as in (6), in which the unreliability $Q = 1 - R$ [25].

$$\begin{aligned} R_{\text{s}} = R_{\text{c}} * \big[& Q_{\text{b}} * (1 - (1 - R_{\text{c}} * R_{\text{b}}^2 * R_{\text{t}})^2) \\ & + R_{\text{b}} * ((1 - Q_{\text{c}}^2) * (1 - (1 - R_{\text{b}}^2 * R_{\text{t}})^2)) \big] \end{aligned} \tag{6}$$

The results of both the analytical and Monte Carlo method are provided in Fig. 3, which shows the system reliability after 3.4 operation years as a function of the sample size N. From this figure can be concluded that the Monte Carlo estimate approaches the analytical reliability of 0.874 when N is larger than 6000 samples. Moreover, in line with the law of large numbers, it is observed that the variability of the reliability estimate reduces with an increase in the sample size.

Further verification of the MC method is obtained by estimating the complete reliability curve of the system $R_s(t)$. The result, provided in Fig. 4, shows that the Monte Carlo estimate with 300k samples accurately approximates the RBD curve throughout the complete lifetime of the system.

III. Case-study Wind Turbine Installation Vessel

In this case study, the proposed MC simulation framework is used to evaluate the reliability of a DC-SPS for a wind turbine installation vessel (WTIV). A WTIV is a dynamic positioning (DP) vessel specifically designed for the fast and cost-effective installation of offshore wind farms [31]. The ship uses a multipurpose tower with an integrated motion compensation system to assemble and install wind turbines on floating or fixed foundations. As the station-keeping ability of the vessel is vital to both the mission and crew safety, the installed SPS must be highly reliable, especially considering the long operation periods at remote locations.

A. System description

As the WTIV is a dynamic positioning vessel of class DPS-3, the propulsion system is required to be fault tolerant against first-order failures, ensuring an uninterrupted station keeping of the ship [32]. The considered power system contains four fire-insulated zones, each connecting to a single generator and two azimuth thrusters, as shown in the power system diagram of Fig. 5. This DC-SPS is modeled along the ring topology and constructed using four MVDC switchboards interconnected through DC transmission lines and circuit breakers. With closed CB operation, the SPS has a ring-like structure around the outside of the vessel to which all electrical loads and generators connect via a PE converter and disconnect switch, in line with [33]. Upon a first-order fault in the SPS, the fault management system can use the CBs to isolate the faulty segment, establishing DP via the three remaining switchboards.

TABLE I
Component reliability indices for the WTIV.

Component reliability index:	Type:	λ in [#/y]		μ in [#/h]	
Transmission line	Active	$\lambda_{t,a}$	0.01	$\mu_{t,a}$	0.125
Converter	Passive	$\lambda_{c,p}$	0.006	$\mu_{c,p}$	1
	Active	$\lambda_{c,a}$	0.006	$\mu_{c,a}$	1
Circuit Breaker	Passive	$\lambda_{b,p}$	0.01	$\mu_{b,p}$	0.25
	Active	$\lambda_{b,a}$	0.01	$\mu_{b,a}$	0.25
	Stuck	f_{cb}	5 %	$\mu_{b,s}$	1

B. Failure rates and modes

For the component failure sampling stage of the MC method, the component reliability indices of Table I are used, in line with [16]. This table provides the failure and repair rates for the active and passive faults in the transmission lines, converters, and circuit breakers. Moreover, the non-tripping of a CB upon exposure to an active failure is modeled as a probability of 5 % ($f_{cb} = 0.05$).

For the reliability analysis, the SPS of the WTIV can be divided into five subsystems, each representing a single function in the ships. Following Fig. 5, the subsystems are defined as the propulsion system, motion compensation system, energy storage system, radar system, and load center. While a system failure of the latter three subsystems is defined by the supply interruption of that module, the failure mode of the propulsion system and motion compensation system is more complex. The propulsion system is considered to be functional if at least 3 out of 4 thruster pairs are connected to the generation modules. In which a thruster pair is attached to the same switchboard (e.g. T_{1a} and T_{4b}). The functionality of the propulsion system is fully defined in (7). The motion compensation system is said

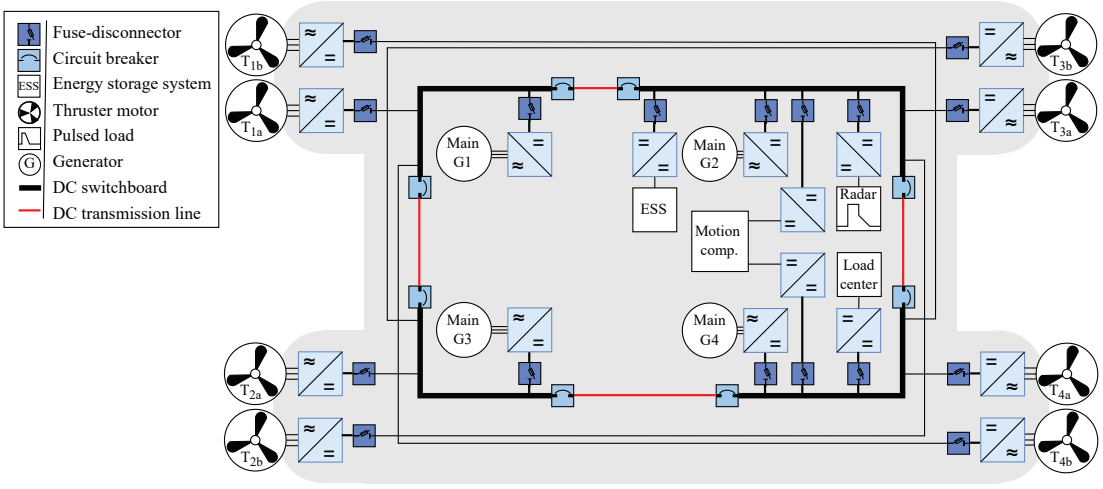

Fig. 5. Meshed DC shipboard power system for the WTIV.

to be functional if it connects to a generation module through either of its two feeders.

$$\text{and}(T_{1a}, T_{4b}) + \text{and}(T_{2a}, T_{3b}) + \text{and}(T_{3a}, T_{2b}) + \text{and}(T_{4a}, T_{1b}) \geq 3 \quad (7)$$

As the functionality of the shipboard power system depends on the performance of the five subsystems, a full SPS failure is said to occur if at least one of the subsystems encounters a fault.

C. Simulation results

The result of the Monte Carlo simulation with 1M samples is provided in Figs. 6 to 9. Fig. 6 shows the estimated reliability curves of the five subsystems and full SPS over an operation period of 50 years. In this figure, it can be observed that the redundant structure for powering the motion composition system significantly enhances the subsystem's reliability when compared to the single-fed load modules. Similar behavior is observed for the propulsion system, which shows high reliability throughout the 50 years of operation due to its single fault tolerance. In contrast, the reliability of the full SPS shows a steep decline, losing over 10 % of its reliability within the first year of operation.

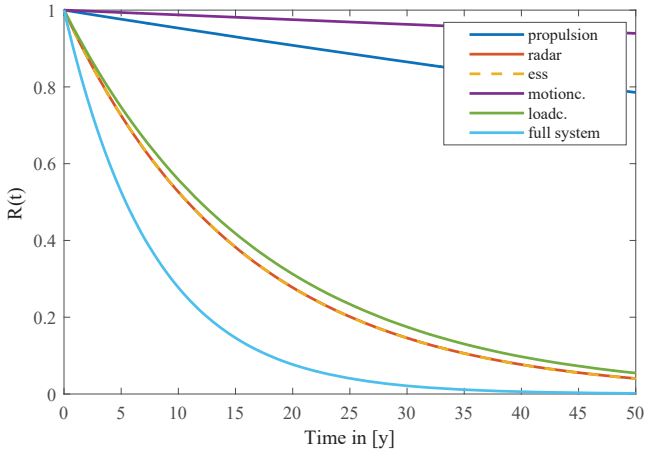

Fig. 6. Simulated reliability curves of the subsystems based on 1M samples.

While the reliability curves of Fig. 6 provide insight into the first supply interruption of the subsystems, a better understanding of the SPS adequacy can be obtained through the analysis of other reliability indices. Fig. 7 provides the estimated failure probability density of the different subsystems after 50 years of operations. In this figure, it can be observed that the full SPS will most likely encounter multiple failures throughout the vessel's lifetime. Meanwhile, the probability that the motion compensation system will experience more than one fault over the 50-year period is less than 0.3 %. To summarize, Table II provides the Monte Carlo estimates for the steady-state service interruption rate and B1 lifetime for all five subsystems and the full SPS.

Another important reliability aspect of the SPS is the average time needed to restore operation after a service interruption. Therefore, the mean time to repair (MTTR) estimates

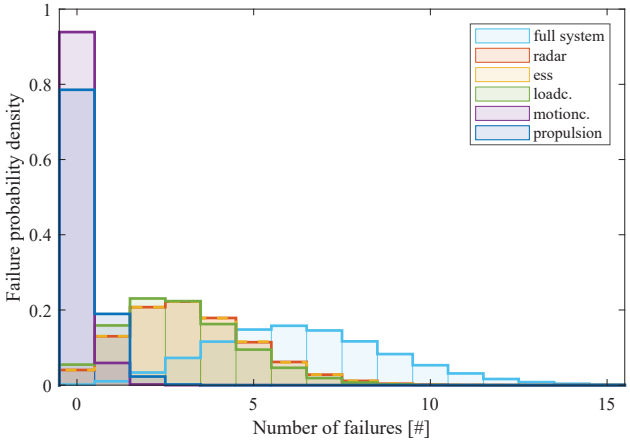

Fig. 7. Simulated failure probability density of the subsystems for a 50y operation time with N = 1M.

TABLE II
STEADY-STATE RELIABILITY INDEX ESTIMATES

Subsystem:	Failure rate:	B1-lifetime:	MTTR:	Availability:
Propulsion	0.551e-6 #/y	2.1 y	0.77 h	99.99996 %
Radar	7.32e-6 #/y	0.16 y	1.9 h	99.99858 %
ESS	7.32e-6 #/y	0.16 y	1.9 h	99.99858 %
Motionc.	0.144e-6 #/y	7.9 y	0.76 h	99.99999 %
Loadc.	6.64e-6 #/y	0.17 y	2.0 h	99.99865 %
Full system	14.6e-6 #/y	0.078 y	1.9 h	99.99716 %

of the Monte Carlo simulation are also provided in Table II. Even though this MTTR gives insight into the restoration characteristics of an average vessel, the distribution of the repair times is lost in the mean value. Hence, Fig. 8 provides the MC estimate for the repair probability density for all five subsystems and the full SPS. It is concluded from this figure that the full SPS, radar system, ESS, and load center all have similar repair characteristics with an average repair time of about 1.9 hours. Meanwhile, this MTTR is more than halved for the subsystem with redundancy.

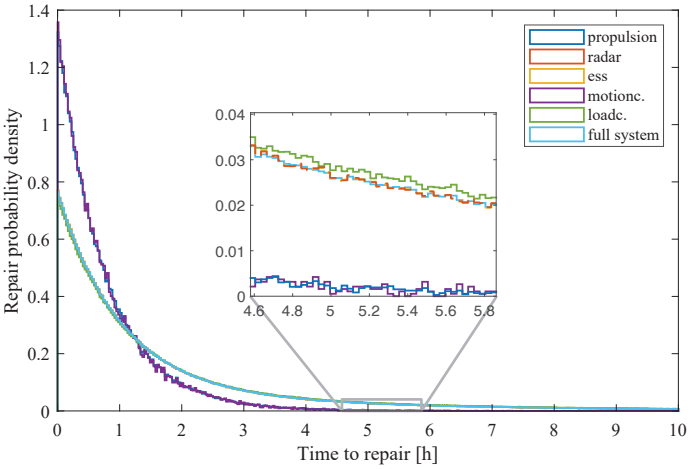

Fig. 8. Simulated repair time distribution of the subsystems with N = 1M.

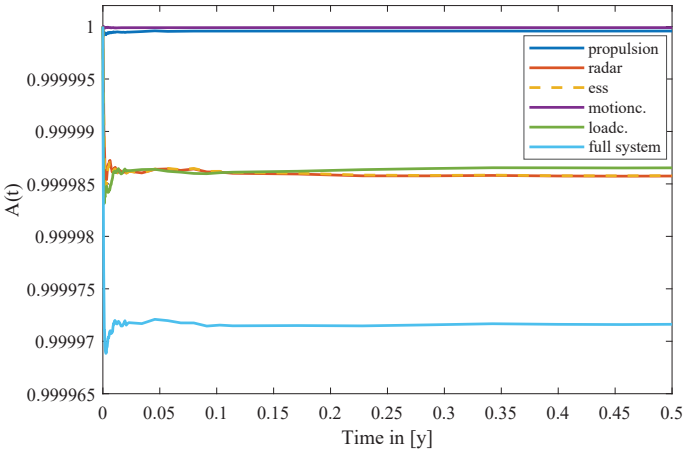

Fig. 9. Simulated availability curve of the subsystems with N = 1M for the first half operation year.

The considered SPS is assumed to be fully functional at time $t = 0\,\text{h}$, achieving an initial availability of 100 %. However, over time, component failures decrease the availability of the system, eventually reaching a constant steady-state value due to the repair of the broken components. To analyze the availability of the shipboard power subsystems, the availability curves are simulated for the first six months of operation using 1M samples. The results, presented in Fig. 9, show that the availability of all subsystems drops from 1 to the steady-state value within the first 150 h of operation. Moreover, it is concluded that the system-level redundancy in the motion compensation and propulsion systems significantly enhances the steady-state availability. The MC estimate of the steady-state availability for the different subsystems is also provided in Table II.

IV. Conclusion

When considering DC shipboard power systems, their reliability is a critical design aspect for both the vessel mission and crew safety. To assess the reliability of DC-SPSs, a Monte Carlo simulation framework was proposed that uses a three-stage structure with component failure sampling, system simulation, and reliability index calculation. This framework was verified for a notional DC shipboard power subsystem and later applied to a ring-type DC-SPS of a wind turbine installation vessel. The results of the MC simulation estimated the stochastic failure behavior of the shipboard power subsystems and provided insight into their repair characteristics. Moreover, the availability of the different subsystems was determined, showing both the dynamic and steady-state behavior. The results revealed that a system-level redundancy in the considered DC-SPS enhances the supply adequacy of the subsystems, increasing its B1 lifetime by over a factor of 40 while reducing the mean time to repair by a factor of 2.5. Overall, the MC simulation showed the strengths and weaknesses of the designed grid, providing a focus for future reliability enhancements.

References

[1] "2023 imo strategy on reduction of ghg emissions from ships," The marine environment protection committee (MEPC), Tech. Rep., 2023.

[2] H. P. Nguyen, A. T. Hoang, S. Nizetic, X. P. Nguyen, A. T. Le, C. N. Luong, V. D. Chu, and V. V. Pham, "The electric propulsion system as a green solution for management strategy of CO2 emission in ocean shipping: A comprehensive review," *International Transactions on Electrical Energy Systems*, vol. 31, no. 11, p. e12580, 2021.

[3] "Maritime technology challenges 2030 - New technologies and opportunities," The European Council for Maritime Applied R&D (ECMAR, Tech. Rep., 2017.

[4] C. Nuchturee, T. Li, and H. Xia, "Energy efficiency of integrated electric propulsion for ships: a review," *Renewable and Sustainable Energy Reviews*, vol. 134, p. 110145, Dec. 2020.

[5] S. Qazi, P. Venugopal, G. Rietveld, T. B. Soeiro, U. Shipurkar, A. Grasman, A. J. Watson, and P. Wheeler, "Powering Maritime: Challenges and prospects in ship electrification," *IEEE Electrification Magazine*, vol. 11, no. 2, pp. 74–87, Jun. 2023.

[6] K. Kim, K. Park, G. Roh, and K. Chun, "DC-grid system for ships: a study of benefits and technical considerations," *Journal of International Maritime Safety, Environmental Affairs, and Shipping*, vol. 2, no. 1, pp. 1–12, Nov. 2018.

[7] L. Qi and J. Lindtjorn, *DC marine vessel electric system design with case studies*, 2021, vol. 143.

[8] Z. Jin, G. Sulligoi, R. Cuzner, L. Meng, J. C. Vasquez, and J. M. Guerrero, "Next-Generation Shipboard DC Power System: Introduction Smart Grid and dc Microgrid Technologies into Maritime Electrical Netowrks," *IEEE Electrification Magazine*, vol. 4, no. 2, pp. 45–57, Jun. 2016.

[9] Y. Song and B. Wang, "Survey on Reliability of Power Electronic Systems," *IEEE Transactions on Power Electronics*, vol. 28, no. 1, pp. 591–604, Jan. 2013.

[10] Baylakoğlu, A. Fortier, S. Kyeong, R. Ambat, H. Conseil-Gudla, M. H. Azarian, and M. G. Pecht, "The detrimental effects of water on electronic devices," *e-Prime - Advances in Electrical Engineering, Electronics and Energy*, vol. 1, p. 100016, 2021.

[11] P. R. Thies, G. H. Smith, and L. Johanning, "Addressing failure rate uncertainties of marine energy converters," *Renewable Energy*, vol. 44, pp. 359–367, Aug. 2012.

[12] A. Dubey and S. Santoso, "Availability-Based Distribution Circuit Design for Shipboard Power System," *IEEE Transactions on Smart Grid*, vol. 8, no. 4, pp. 1599–1608, Jul. 2017.

[13] A. Vicenzutti, R. Menis, and G. Sulligoi, "All-Electric Ship-Integrated Power Systems: Dependable Design Based on Fault Tree Analysis and Dynamic Modeling," *IEEE Transactions on Transportation Electrification*, vol. 5, no. 3, pp. 812–827, Sep. 2019.

[14] A. Dubey, S. Santoso, and A. Arapostathis, "Reliability analysis of three-dimensional shipboard electrical power distribution systems," in *2015 IEEE Electric Ship Technologies Symposium (ESTS)*, Jun. 2015, pp. 93–98.

[15] H. Jiang, C. H. Peng, and J. Xiao, "Reliability analysis for the power system of the nuclear ship Savannah," *Journal of Physics: Conference Series*, vol. 2208, no. 1, p. 012003, Mar. 2022.

[16] B. Stevens, A. Dubey, and S. Santoso, "On Improving Reliability of Shipboard Power System," *IEEE Transactions on Power Systems*, vol. 30, no. 4, pp. 1905–1912, Jul. 2015.

[17] Z. Wang, S. Karimi, M. Zadeh, and M. Heimdal, "Reliability Modelling of Marine Hybrid Power and Propulsion System Considering Operation Profile," in *2023 IEEE International Conference on Electrical Systems for Aircraft, Railway, Ship Propulsion and Road Vehicles & International Transportation Electrification Conference (ESARS-ITEC)*. Venice, Italy: IEEE, Mar. 2023, pp. 1–6.

[18] R. Menis, A. da Rin, A. Vicenzutti, and G. Sulligoi, "All electric ships dependable design: Integrated power system analysis using dynamic reliability block diagram," in *Marine Electrical and Control Systems Safety Conference (MECSS)*, 2013.

[19] W. Li *et al.*, *Reliability assessment of electric power systems using Monte Carlo methods*. Springer Science & Business Media, 2013.

[20] A. Rei and M. Schilling, "Reliability Assessment of the Brazilian Power System Using Enumeration and Monte Carlo," *IEEE Transactions on Power Systems*, vol. 23, no. 3, pp. 1480–1487, Aug. 2008.

[21] B. Zhang, M. Wang, and W. Su, "Reliability Analysis of Power Systems Integrated With High-Penetration of Power Converters," *IEEE Transactions on Power Systems*, vol. 36, no. 3, pp. 1998–2009, May 2021.
[22] J. Hedel and A. Abuelrub, "Reliability Assessment of Protection System for DC Ring Microgrid Using Fault Tree Method," in *2020 7th International Conference on Electrical and Electronics Engineering (ICEEE)*, 2020, pp. 106–110.
[23] X. Shi and A. M. Bazzi, "Fault tree reliability analysis of a micro-grid using Monte Carlo simulations." Champaign, IL, USA: IEEE, Feb. 2015, pp. 1–5.
[24] L. Xu, S. Gao, and X. Zhao, "Reliability Evaluation for a Grid Connected Offshore Wind Farm," in *2020 IEEE 4th Conference on Energy Internet and Energy System Integration (EI2)*. Wuhan, China: IEEE, Oct. 2020, pp. 3181–3186.
[25] R. Billinton and R. N. Allan, *Reliability evaluation of engineering systems*. Springer, 1992, vol. 792.
[26] B. W. Tuinema, J. R. Torres, A. I. Stefanov, F. M. Gonzalez-Longatt, and M. van der Meijden, *Probabilistic Reliability Analysis of Power Systems*. Springer, 2020.
[27] S. Peyghami, Z. Wang, and F. Blaabjerg, "Reliability Modeling of Power Electronic Converters: A General Approach," in *2019 20th Workshop on Control and Modeling for Power Electronics (COMPEL)*. Toronto, ON, Canada: IEEE, Jun. 2019, pp. 1–7.
[28] M. Novak, A. Sangwongwanich, and F. Blaabjerg, "Monte Carlo-Based Reliability Estimation Methods for Power Devices in Power Electronics Systems," *IEEE Open Journal of Power Electronics*, vol. 2, pp. 523–534, 2021.
[29] F. M. Dekking, C. Kraaikamp, H. P. Lopuhaä, and L. E. Meester, *A Modern Introduction to Probability and Statistics: Understanding why and how*. Springer, 2005, vol. 488.
[30] B. Amanulla, S. Chakrabarti, and S. N. Singh, "Reconfiguration of Power Distribution Systems Considering Reliability and Power Loss," *IEEE Transactions on Power Delivery*, vol. 27, no. 2, pp. 918–926, Apr. 2012.
[31] Z. Jiang, "Installation of offshore wind turbines: A technical review," *Renewable and Sustainable Energy Reviews*, vol. 139, p. 110576, Apr. 2021.
[32] American Bureau of Shipping, "Guide for dynamic positioning systems," Tech. Rep., 2021.
[33] "Ieee recommended practice for 1 kv to 35 kv medium-voltage dc power systems on ships," *IEEE Std 1709-2018 (Revision of IEEE Std 1709-2010)*, pp. 1–54, 2018.